

**Fig. 1.** Trajectory of comet ISON across the SUMER FOV in the SOHO coordinate system (units of arcseconds). SOHO's attitude is oriented toward ecliptic north. For each minute the predicted position of the central brightness is marked by a dot. The accessible FOV of SUMER – here indicated by a dashed line – refers to the central pixel of the slit. The instantaneously imaged area of  $200'' \times 240''$  is just inside the LASCO-C2 occulter (dash-dotted circle).

Comet 2012/S1 (ISON) – believed to originate from the Oort Cloud and approaching the Sun in a sungrazing orbit – is a very special case that excited the community, but also left it with a bundle of question marks. The lack of comparable events in the past spawned non-converging predictions and wild speculations. It was clear that ISON, coming as close as  $2.7 R_{\odot}$  to the Sun, would offer a unique chance for cometary science and in particular for spectroscopy. Oort-Cloud comets are ideal objects to study compositional information and outgassing processes, and a worldwide campaign was initiated to observe the comet in various bands of the electromagnetic spectrum (e.g., Knight et al., 2014; Druckmüller et al., 2014; Agúndez et al., 2014). Yet, ground-based night-time telescopes and instruments in near-Earth-orbit often have limitations when they are pointed close to the Sun. ISON, however, came so close that solar telescopes were able to close that gap.

## 1. Observations: images and spectra

Even early orbit predictions showed that ISON's trajectory would cross the field-of-view (FOV) of the Solar Ultraviolet Measurements of Emitted Radiation (SUMER; Wilhelm et al. 1995) spectrometer on SOHO during perihelion transit, offering a unique chance of high-resolution spectroscopic observations at far-ultraviolet (FUV) wavelengths. We transformed the latest ephemerides (JPL orbital elements set #54) to SUMER coordinates using the attitude and orbit information of SOHO. Figure 1 depicts the comet trajectory across the SUMER FOV in SOHO coordinates from a start position  $x=-894''$ ,  $y=-1768''$  to a final position  $x=-1644''$ ,  $y=701''$  imposed by the mechanism limits. Each dot in Fig. 1 stands for the predicted position of the central brightness at a given minute. The comet was expected to enter the FOV at 17:56 UTC.

We completed limb tests to improve the pointing accuracy and assumed that the uncertainty is  $\approx 5''$  in azimuth and  $\approx 10''$  in elevation. The uncertainty of the orbit prediction is even smaller (Giorgini 2014, private communication).

**Images:** first, SUMER was operated in slot mode, that is, with a 2 mm hole instead of the slit. In this mode, the telescope provides 2D stigmatic images that are in  $x$ -direction convolved with the  $\text{Ly-}\alpha$  line profile. From each exposure of 15 s a window of  $200 \text{ px} \times 240 \text{ px}$  was flatfield-corrected on board and downlinked in real time with a  $2 \times 2$  pixel binning.

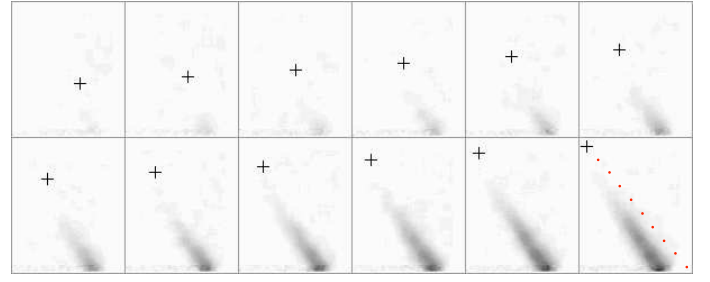


**Fig. 2.** Dust tail of comet ISON around perihelion transit observed in  $\text{Ly-}\alpha$ . These 12 slot images with a size of  $200'' \times 240''$  were taken with a cadence of 30 s between 17:56 and 18:01 UTC (top left to bottom right). The cross marks the predicted position of the nucleus. In the final image red dots indicate the trajectory in steps of 30 s.

Altogether, 101 images were obtained in this mode. The first 70 images show no cometary signal. We calculated an average background image from these images for straylight subtraction in the remaining images. Finally, a median 10 filter was applied for noise reduction. In Fig. 2 a series of 12 images – each one the sum of two exposures – shows the entry of the comet into the SUMER FOV. The orbit was almost tangential at that time, and distance to perihelion was only  $0.15 R_{\odot}$ . A cross in each image marks the predicted position of the nucleus. The granulation along the feature is most likely an artifact, a combination of residual detector inhomogeneity and noise-filtering. The noise in the bottom pixels stems from an edge problem of the noise filter.

**Spectra:** at 18:02 UTC the slit-less sequence was stopped and the spectroscopic mode started, employing the  $4''$  slit. The prime goal of this mode was the spectroscopic analysis of gas and plasma emission in the coma and gaining compositional information. Our sequence cycled through four spectral windows around 105 nm, 110 nm, 121 nm, and 131 nm, chosen for emission lines of molecules, atoms, and ions such as O VI. We re-pointed every ten minutes to track the comet. However, most of these spectra had an extremely low signal, only few spectra showed signal of scattered light from the solar disk. We can exclude that emission of cometary gas or plasma above detection limit was recorded then. The lack of any signature in SDO-AIA images corroborates this finding.

### 1.1. Comet morphology

The very short ionization time of neutral hydrogen so close to the Sun sets an upper limit to the extent of the neutral hydrogen coma in  $\text{Ly-}\alpha$  at a few 100 km, well within one SUMER pixel. Moreover, the number of hydrogen atoms in the  $\text{Ly-}\alpha$  emission state is also reduced by orders of magnitude (compared to a similar case farther away from the Sun) as our Haser calculations have shown. Such considerations also apply for other gaseous species, thus excluding emission from genuine neutrals as well as from charge-exchange neutrals (Bemporad et al. 2005). Hence, the measured radiance is attributed to sunlight that is reflected and scattered by the cometary dust, since thermal emission of the dust at FUV wavelengths is negligible.

The  $\text{Ly-}\alpha$  emission above background level shows a spiky diffuse arrow-shaped coma with a tip in ram direction. No local brightness condensation or any other indication of the nucleus is found above detection limit. The spiky coma lags behind the predicted position. Pointing uncertainty and orbit prediction uncertainty cannot explain this discrepancy. The coma and tail re-

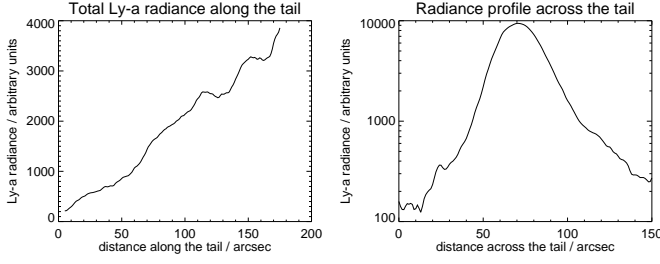


**Fig. 3.** Radiance profile of the coma along and across the tail.

gion is offset from the expected trajectory in antisolar direction and appears at a small angle to the comet path. The brightness increase along the feature is approximately linear from the tip to maximum level close to the edge of the image (see Figs. 3 and 4a). The slope of the brightness increase is about 1.7 relative units per 100 Mm. The elongated coma extends over at least 240 Mm with a possible peak brightness at or beyond the lower edge of the image. The core isophotes of the coma spike are symmetric with respect to the main axis of the coma pattern. This main axis is rather straight and is oriented along a position angle  $PA$  of  $72^\circ$  with respect to celestial North. The lower level isophotes are asymmetric with respect to this line and appear to be more extended in the direction of the Sun. The spiky coma has an opening angle of about  $13^\circ \pm 1^\circ$  as seen from the front end tip and reaches a maximum width of more than 100 Mm. Figure 4a depicts an enlarged copy of the last image in Fig. 2. Again, the cross marks the predicted position of the nucleus at mid-exposure, and ten red dots mark its position at one-minute intervals. It is obvious that the tail is offset from the trajectory by  $\approx 30''$  in a direction away from the Sun. This is three times more than the pointing uncertainty. We also studied the cross-section of the tail. At ten positions we determined the geometrical center of brightness across the tail. In Fig. 4a these locations are marked by white dots. The bi-sector – the line connecting these dots – is not aligned with the trajectory, but appears at an angle of  $\approx 5^\circ$  in anti-solar direction from the trajectory. It does not seem to be a perfect straight line either but has a curvature toward the suspected nucleus position.

## 1.2. Radiometry

Scattered light from the disk limits the detectability of off-disk targets in unocculted solar telescopes. At the comet's position – far out at the edge of the SUMER FOV – Ly- $\alpha$  radiation of the disk produces a scattered-light level that is four orders of magnitude lower than that of the average quiet Sun (Curdt et al. (2001)). The measured Ly- $\alpha$  background of  $19.3 \text{ mW}/(\text{m}^2 \text{ sr})$  is similar to the radiance emerging from the coma, which is  $18 \text{ mW}/(\text{m}^2 \text{ sr})$  in the brighter sections. Since we observed at a short wavelength of  $121.6 \text{ nm}$ , we assume that a geometric model can be used for estimating the dust column density for  $\mu\text{m}$ -sized particles. For an optically thin dust environment, the radiance of the dust tail,  $L_{\text{tail}}$ , is given by

$$L_{\text{tail}} = A \eta l \pi r^2 L_{\text{disk}},$$

where  $A$  denotes the phase-angle-dependent albedo,  $\eta$  the volumetric density of the particles,  $l$  the column length,  $r$  the dust grain radius, and  $L_{\text{disk}}$  the average radiance of the solar disk. For simplification we assumed both of the latter to be uniform. The Sun was extremely quiet during perihelion transit, its irra-

diance was only 11% above solar minimum levels<sup>1</sup>. Therefore, we can assume a solar radiance  $L_{\text{disk}}$  of  $\approx 101 \text{ W}/(\text{m}^2 \text{ sr})$ . With a column length of  $\approx 10''$  – equivalent to  $7.25 \text{ Mm}$  – and the tail being  $1.8 \cdot 10^{-4}$  times fainter than the disk, the product  $A \eta \pi r^2$  can be determined. For an example case with a value of 0.1 for the albedo and a standard grain radius of  $10 \mu\text{m}$  a result of  $\approx 0.78$  particles /  $\text{m}^3$  for  $\eta$  is returned. This implies that in total  $\approx 2.7 \cdot 10^{21}$  standard grains are in the observed structure, equivalent to a volume of  $1.15 \cdot 10^7 \text{ m}^3$  or a mass of  $11.500 \text{ t}$  of material with unit density.

In the latest C2 images the shape of the comet is also pin-tipped (cf., Fig. 3 in Druckmüller et al., 2014). Despite this similarity, we were unable to reliably determine the same ratio for visible-light to further constrain the grain size distribution. Coalignment of images that are neither cospatial nor cotemporal is problematic, and C2 data at altitudes  $\leq 3R_\odot$  have significant photometric uncertainties (Knight et al. 2010).

## 2. Coma and tail modeling

We employed dust dynamic models to reproduce the main features observed. Finson-Probstein calculations (Finson & Probstein 1968; Beißer 1991) show that the main axis of the coma spike with a position angle  $PA$  of  $72^\circ$  follows a synchrone with an emission time at  $8.5 \text{ h} \pm 0.5 \text{ h}$  before perihelion transit. The narrow opening angle of the coma spike ( $\approx 13^\circ$ ) covers synchrones of dust that might have been emitted within at most 12 h before perihelion transit. We thus assume that the coma pattern seen in SUMER images resulted from a short dust-emission event less than half a day before. The dust production of the event decayed rapidly within a few hours. As a consequence, one has to assume that the nucleus of the comet is located close to the tip of the coma spike. The extension of the main spike axis covers dust with a ratio  $\beta$  for the solar radiation pressure to solar gravity of up to 0.025, representative of basaltic dust of a few  $\mu\text{m}$  size and larger, or graphite grains larger than  $10 \mu\text{m}$ . We note that basaltic-type grains of very small size ( $< 0.02 \mu\text{m}$ ) may have similar  $\beta$  ratios, but appear to be inefficient light scatterers at FUV wavelength.

The dust coma of a continuously active comet usually appears roundish with a typical diameter of several 10 Mm and a pronounced brightness peak close to the center that accommodates the nucleus. For comet ISON such a coma pattern with a diameter of  $> 150''$  and a sharp brightness falloff at its front was seen in LASCO images until shortly before the extreme brightening on Nov 28. This changed after the final brightening, the tail head narrowed continuously and became almost pin-like, comparable in width to a C2 pixel of  $11.4''$  with no sharp edge at the tail head anymore when it disappeared behind the C2 occulter. The arrow-shaped spiky dust coma evolved immediately after the brightness maximum. Brightness outbursts of several magnitudes normally indicate nucleus fragmentation events (Boehnhardt 2004). An extraordinary brightness peak with a maximum of -2 to -3mag was measured in comet ISON on Nov 28 between 0 and 7 UTC (Knight & Battams 2014). Additional indications for extraordinary dust production around that time period come from the preliminary analysis of the post-perihelion dust tail of comet ISON (Boehnhardt 2013; Sekanina et al. 2013). It is very unlikely that the observed spiky coma in SUMER and LASCO images is produced by a chain of active nucleus fragments from the Nov 28 break-up. Typical separation speeds from known nucleus splittings amount to less than

<sup>1</sup> <http://lasp.colorado.edu/lisird/lya/>

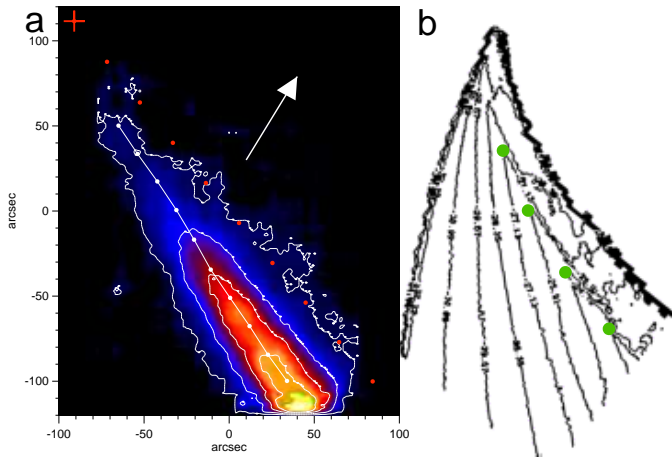


**Fig. 4. a:** Zoom of the last image in Fig. 2. The bi-sector of the tail is indicated by a white line. Predicted positions of the nucleus at mid-exposure for the last 10 minutes are shown as red dots (ending with a cross) and indicate the trajectory. The arrow points toward Sun center. The tail is offset from the trajectory and not parallel to it. **b:** A model dust tail can reproduce the observation. The line of green dots marking the tip points of the higher-level contours resembles the tail axis, if we assume a violent dust emission burst  $\approx 8.5$  hours prior to perihelion transit followed by a sharp decrease of the dust production.

10 m/s, which is insufficient for the extension of the coma spike in comet ISON (Boehnhardt 2004). One would have to assume separation speeds of several km/s.

In a trial-and-error approach we used the Cosima dust simulation software (BeiBer 1991) to model dust-tail images and isophote patterns in comet ISON for the SUMER observing period with the goal to quantitatively describe the scenario outlined above and to obtain further conclusions on the event and the released dust. With a continuous dust production rate we were unable to reproduce anything similar to what was observed. The simulations show that an arrow-shaped coma with a position angle of  $72^\circ$  for the main axis of the isophotes results for decreasing dust activity after about 8h before perihelion transit (see Fig. 4b). The main axis is offset by about 20 Mm to 30 Mm (projected into the sky) from the nucleus trajectory in antisolar direction. The brightness gradient in the coma spike is reproducible for a fast activity drop by two orders of magnitude within 3 h to 5 h after the break-up time (which also defines the period of main dust production). Knight & Battams (2014) also postulated such a behavior in their preliminary analysis. The dust expansion velocity is constrained by the opening angle of the coma spike to extend not more than  $\approx 0.5$  km/s (which results in an opening angle of  $12^\circ$ , while a dust expansion speed of 2 km/s would result in an angle of  $\approx 17^\circ$ ).

### 3. Discussion

We interpret the coma and tail appearance of the comet shortly before perihelion transit as an indication for a rapid decrease of dust production, which had ceased or dropped drastically by the time the comet entered the SUMER FOV, not showing any visible signature of on-going activity. Although taken at a different wavelength and at a much higher resolution, the appearance of the tail in Fig. 4a can be understood as a continuation of the dimming and narrowing process observed in LASCO C2 that finally leads to a complete disappearance of nucleus activ-

ity. Interestingly, similar effects were reported by Bonev et al. (2002) when they observed the disintegration of comet C/1999 S4 (LINEAR), although this process occurred at a much larger distance from the Sun and took several days to complete. The effects observed at comet ISON during its last hours of activity seem to be similar, although much more accelerated.

Micron-sized and possible larger dust fills an arrow-shaped coma with a linear slope of surface brightness in motion direction. This coma pattern can be understood as a consequence of a rapidly decaying (few hours) dust activity after a major nucleus break-up event that occurred about 8.5 h (and definitely less than 12 h) before perihelion transit of the comet, that is, after maximum brightness in the outburst on Nov 28. It may thus represent the dusty aftermath of this nucleus splitting. Most of the solids released during the outburst and before may have disappeared. This might be due to evaporation of dust material in the very hot environment close to the Sun where grains may have to experience temperatures of up to 2000 K.

The low-level Ly- $\alpha$  flux of the dust coma is slightly asymmetric with respect to the main spike axis, with a larger extension on the sunward side. This finding is not represented in the isophote patterns of the dust coma simulations of the event as described above. We note, however, that the enhanced low-level activity covers the trajectory path of the nucleus through our FOV. Therefore one can assume that additional dust exists on the sunward side of the arrow-shaped coma from the ceasing activity of the comet. This dust is unrelated to the possibly fatal break-up of the comet around Nov 28 at 10:15 UTC, but results from earlier activity of the nucleus. Given its low intensity, the dust may be subject to evaporation with significantly higher mass loss than at its release epoch.

### 4. Conclusion

Unfortunately, the comet made it impossible to reach our prime scientific goal, and no compositional information was obtained. However, we managed to observe ISON's coma in Ly- $\alpha$  emission only minutes before perihelion transit, when other instruments were paused because of the close proximity of the solar disk. We interpret the signal as scattered light from the disk, resembling a -8.5 h synchrone, and were able to model a tail with a spiky coma and brightness decrease in motion direction, and with the nucleus not embedded in the dust cloud.

Our dust dynamic model definitively requires a sharp fall-off of the dust production hours before perihelion transit. Therefore our observations clearly indicate that the dust production had already stopped before the comet entered our FOV and that only the relicts of previous activity are seen.

The Ly- $\alpha$  radiance of the dust tail was four orders of magnitude below the disk radiance, not too far from the detection limit of our instrument. An enormous dynamical range is required for instruments that observe the comet together with the disk. This may explain why no signature of the comet was seen in SDO-AIA data.

The SUMER Ly- $\alpha$  images of comet ISON, taken within an hour from perihelion transit, are unique and show the cometary dust coma produced under very unusual circumstances. To our knowledge, such observations have never been completed before. They complement observations by other instruments, and their scientific value has to be seen in concert with these other observations.

*Acknowledgements.* W.T. Thompson provided us with HPC coordinates as seen from SOHO. An exceptional effort of D. Germerott and the SOHO flight opera-

tions team was required for this time-critical observation. We received very constructive comments from an anonymous referee. The help of all of them is greatly acknowledged. The SUMER and LASCO projects are financially supported by DLR, CNES, NASA, and the ESA PRODEX Programme (Swiss contribution). SUMER and LASCO are part of SOHO of ESA and NASA.

## References

- Agúndez, M., Biver, N., Santoz-Sanz, P., Bockelée-Morvan, D., & Moreno, R. 2014, A&A **564**, L2.
- Beißer, K. 1989, RvMA **2**, 221.
- Beißer, K. 1991, Astr. Nachr. **312**, 223.
- Bemporad, A., Poletto, G., Raymond, J.C. et al., 2005, ApJ **620**, 523.
- Boehnhardt, H. 2004, in (eds. Festou, Keller, Weaver) '*Comets II*', Univ. Arizona Press, Tucson, 301.
- Boehnhardt, H. 2013, CBET **3715**, 1.
- Bonev, T., Jockers, K., Petrova, E., Delva, M., Borisov, G., & Ivanova, A. 2002, Icarus **160**, 419.
- Curd, W., Brekke, P., Feldman, U., et al., 2001, A&A **375**, 591.
- Druckmüller, M., Habbal, S.R., Aniol, P., Ding, A., & Morgan, H. 2014, ApJL **784**, L22.
- Finson, M. & Probst, R. 1968, ApJ **154**, 327.
- Knight, M.W., A'Hearn, M.F., Biesecker, D.A., et al. 2014, ApJ **139**, 926.
- Knight, M.W. & Battams, K. 2014, ApJL **782**, L37.
- Sekanina, Z., Marcus, J.M., Battams, K. 2013, CBET **3722**, 1.
- Wilhelm, K., Curd, W., Marsch, E., et al., 1995, Sol. Phys. **162**, 189.